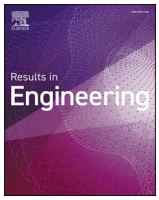
Results in Engineering 19 (2023) 101231



Contents lists available at ScienceDirect

Results in Engineering

journal homepage: www.sciencedirect.com/journal/results-in-engineering



Application of the modified capacitance-resistance method to model reservoir pressure maintenance

Ali Lesan [a], Reza Shams [b], Peyman Pourafshary [c,*], Abbas Bahrodi [a], Hosna Rastkerdar [d]

[a] College of Engineering / School of Mining Engineering, University of Tehran, Tehran, Iran
[b] Department of Chemical and Petroleum Engineering, Sharif University of Technology, Tehran, Iran
[c] School of Mining and Geosciences, Nazarbayev University, Astana, Kazakhstan
[d] Department of Reservoir Engineering, Faculty of Petroleum and Chemical Engineering, Science and Research Branch, Islamic Azad University (IAU), Tehran, Iran

ARTICLE INFO

Keywords:
Capacitance-resistance model
Aquifer
Pressure maintenance
Water injection

ABSTRACT

A pressure maintenance strategy is crucial in reservoir management, especially in single-phase oil reservoirs, to keep the reservoir pressure above the bubble point. Water injection is a common way to prevent pressure decline due to production. Water may be injected into oil zone and/or aquifer. Analytical and semi-analytical methods are applied to analyze the reservoir response and pressure alteration during the water injection and pressure maintenance operation. Capacitance- Resistance Model (CRM) is a well-known semi-analytical method to predict oil production by water flooding.

In this work, Static Capacitance- Resistance Model (SCRM) in which time constant parameter is unique value in whole matching duration has been applied to estimate water injection in the reservoirs with charging aquifer; in addition to, our aim is analytical investigation of water injection performance in the aquifer zone. As a matter of fact, SCRM has been coupled for the reservoir and aquifer in which SCRM has been written for a reservoir and an aquifer zone as two independent porous medium. Consequently, SCRM has been developed to estimate pressure maintenance performance in the cases of charging aquifer; moreover, new parameter is defined as pressure difference between aquifer and reservoir transition zone (DP) is added to SCRM tuning parameters that can indicate flow and reverse flow between reservoir and aquifer.

This parameter is a water saturation-dependent function considered as another tuning parameter. Two synthetic reservoirs were simulated in this work, including homogenous and streak cases with nine spot patterns. The developed SCRM has shown acceptable accuracy, of which 6.1% of total absolute error was obtained for the homogenous case and 7.5% for the streak case.

1. Introduction

Water flooding, the oldest and most common oil recovery method, increases the displacement efficiency in a reservoir and maintains its pressure. Appropriate selection of injection rates and injection patterns during a water flooding project is essential in operational and economical decisions for reservoir managements. As a secondary recovery approach, water injection analysis has been conducted either numerically or semi-analytically. Commercial simulators' common numerical solutions are time-consuming and complicated due to the data requirements and uncertainties; therefore, it is vital to reduce complexity with more straightforward approaches with acceptable accuracy [1–3]. Semi-analytical approaches are faster in alleviating complexity in reservoir models. One of the most famous approaches to estimate injection performance is the Capacitance Resistance Model (CRM). This model has inspired from the electrical circuit that was presented in 1943. The CRM semi-analytical approach simulates reservoir performance using available injection/production data as input values [4]. CRM has a synchronized reservoir to an electrical circuit in which each reservoir parameter has an equivalent meaning in an electrical circuit, such as resistance and capacitance. CRM can estimate the reservoir performance using these two parameters with acceptable accuracy. CRM was adopted to state well connectivity for injectors and producers' network by considering injections as input signals and productions as output signals [5,6]. By estimating connectivity, water flooding performance can be estimated [7,8]. The parameter f is also

* Corresponding author.
E-mail address: peyman.pourafshary@nu.edu.kz (P. Pourafshary).

https://doi.org/10.1016/j.rineng.2023.101231
Received 25 April 2023; Received in revised form 9 June 2023; Accepted 11 June 2023
Available online 20 June 2023
2590-1230/© 2023 The Authors. Published by Elsevier B.V. This is an open access article under the CC BY-NC-ND license (http://creativecommons.org/licenses/by-nc-nd/4.0/).

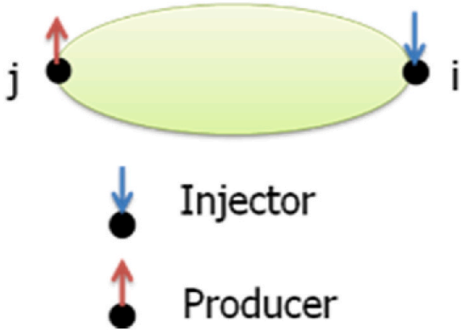


Fig. 1. CRMT control volume.

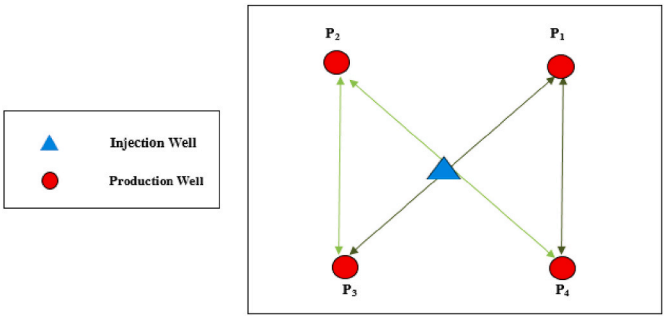


Fig. 2. CRMP control volume.

known as inter well connectivity, gain, or injection allocation factor to account for the effects of leakage (f < 1) and aquifer pressure support (f > 1) [9,10]. Bottom hole pressure also affects the production during water flooding and should be considered in the model [11]. The dependency of an output response (production) to the time-dependent input (injection) is characterized as a time constant in the model solution to simulate injection/production interactions. The time constant term (denoted by τ) shows the reservoir storage characteristic [12,13]. Semi-analytical solution for the CRM has been derived for different control volumes such as tank, one injector/producer pair, and a group of injectors/producers [4,8] to model various conditions during gas or water flooding operations [14–21]. By estimating connectivity and time constant values, the main petrophysical structure of the reservoir can also be characterized by CRM [22–26]. The reservoir performance predicted by CRM should be correlated with economical factors to design an efficient operation [27]. Some developments have been applied to CRM to improve the applicability for more complex conditions. For instance, CRM is applied to multilayer reservoirs to evaluate reservoir performance [28]. CRM has been also coupled with geomechanical equations [29–31]. CRM has been applied to characterize fractures induced by the thermal process [32]. Comparison between CRM and streamline allocation approach has been done where results show more reliable results for the long-distance injector-producer. CRM has been developed to simulate tracer flow [33], carbon sequestration [34], zonal intelligence [35], well control [36], and smart field modeling [37]. Matrix format was derived for CRM [38]. A stochastic approach has been adopted to improve reservoir management efficiency [13]. Some novel approaches have been implemented to estimate miscible injection performance that can broaden new horizons to complete CRM applications [39]. Recently, the error effect on CRM is being developed to promote CRM reliability [40]. Currently, research on going to couple CRM as a semi analytical approach with neural network and machine learning approaches [41,42]. To improve the accuracy of CRM, a new approach was developed to consider variable time constant parameter during production [43]. Still, a static CRM (SCRM) with a fixed time constant provides acceptable simulation results in most approaches. For example, SCRM is applied to evaluate pressure maintenance behavior during water injection at the aquifer and couple aquifer performance with the reservoir [44,45]. More development is required to mathematically modify SCRM equations for aquifer and aquifer/reservoir coupling to estimate the reservoir performance charging with an aquifer accurately. In this work, SCRM has been applied for two continuous porous media. The first porous medium has been considered as an aquifer and the second one has been made equivalent to an undersaturated oil reservoir with water drive recovery mechanism. This new approach helps to characterize aquifer and predict water influx to reservoir, which is important in designing a reservoir management strategy.

2. Methodology

This section illustrates concepts of aquifer/reservoir modeling by the SCRM approach.

2.1. Fluid flow in reservoir model

Aquifers provide the main energy to produce oil in the primary recovery period in water drive reservoirs. Water drive reservoirs with strong aquifer support are known by gradual pressure decline and the highest primary recovery factor. Water is injected into the aquifer to enhance pressure maintenance in weaker supports. Fluid flow in aquifers is classified as steady state/pseudo steady-state and unsteady state. Adding aquifer effect to the conventional SCRM is challenging due to the lack of data from the aquifer fluid flow.

In our approach, aquifers are assumed to be finite porous media, where wells are drilled to control the pressure drop. Hence, a gradual pressure drop occurs in the aquifers, which makes applying the pseudo steady state aquifer model reasonable. Flow stream, storage capacity in porous media, pressure difference, and permeability are modeled similar to electrical current, capacitance, potential difference, and resistance.

The conventional CRM approach is used to model the fluid flow in the reservoir. The following general mass balance can be written for the reservoir.

$$V_{pr}C_{tr}\left(\frac{d\bar{p}}{dt}\right) = i(t) - q(t) \tag{1}$$

Equation (1) shows CRM main equation in the reservoir in which V_{pr} is reservoir pore volume, C_{tr} is reservoir total compressibility, $\frac{d\bar{p}}{dt}$ is reservoir average pressure changing by time, $i(t)$ is injection rate and $q(t)$ is production rate. It can be inferred that this equation including single injection and production well (Fig. 1), which is named CRMT [4]:

If the reservoir contains multiple injection and production wells like Fig. 2; Equation (1) changes into Equation (2) in which f_{ij} is the weight coefficient for each pair of injectors and producers. This case is named as CRMP [4].

$$V_{pr}C_{tr}\left(\frac{d\bar{p}}{dt}\right) = \sum_{i=1}^{N_i} f_{ij}i_i(t) - q_j(t) \tag{2}$$

If J is considered as productivity index, q production rate, $\bar{p}$ average reservoir pressure and p_{wf} well flow pressure(bottom hole pressure), linear productivity index equation $q = j(\bar{p} - p_{wf})$ can be adopted to make connection between reservoir mean pressure and production rate; consequently, reservoir mean pressure in Equation (2) will be replaced by production rate and CRMP is reformed as Equation (3)

$$\frac{C_{tr}.V_{pr}}{j}.\frac{dq}{dt} + q(t) = \sum_{i=1}^{N_i} f_{ij}i_i(t) - C_{tr}.V_{pr}.\frac{dP_{wf}}{dt} \tag{3}$$

Where $\tau_r = \frac{C_{tr}.V_{pr}}{J}$ is named reservoir time constant or lag time. After solving the differential Equation (3); Equation (4) will be yielded:

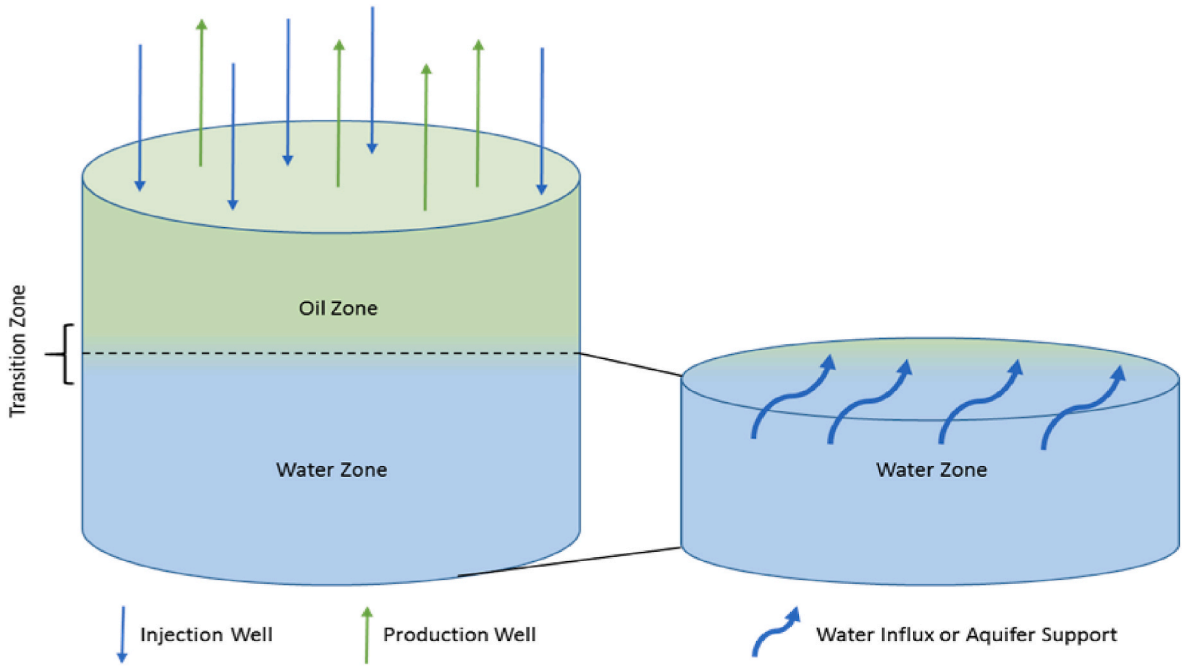


Fig. 3. Injection- Production network for water drive reservoir.

$$q_j(t_n) = q_j(t_0)e^{-\left(\frac{t_n - t_0}{\tau_j}\right)} + \sum_{i=1}^{N_i}\left[f_{ij}\left(i_i(t_n) - e^{-\left(\frac{t_n - t_0}{\tau_j}\right)} i_i(t_0)\right)\right] - \sum_{k=1}^{n}\left\{\tau_j e^{-\left(\frac{t_n - t'_k}{\tau_j}\right)}\left(1 - e^{-\left(\frac{\Delta t_k}{\tau_j}\right)}\right)\left[\sum_{i=1}^{N_i} f_{ij}\frac{\Delta i_i^{(k)}}{\Delta t_k} + J_j\frac{\Delta P_{wf}^{(k)}}{\Delta t_k}\right]\right\} \quad (4)$$

SCRM (Equation (4)) could estimate immiscible injection performance with two tuning parameters mentioned before including τ_j time constant of producer and f_{ij} is connectivity of producer number j and injector number i. This equation should be modified to consider the effect of water encroachment from aquifers in water drive formations.

2.2. SCRM development for an aquifer/reservoir system

Equation (5) shows the basic material balance equation for an aquifer connected to a reservoir, as shown in Fig. 3.

$$C_{taquifer}.V_{p_{aquifer}}\left(\frac{d\overline{p}_{aquifer}}{dt}\right) = \sum_{i=1}^{N_i}\lambda_{ij}i_i(t) - e_w(t) \quad (5)$$

Where $C_{taquifer}$ is the total aquifer compressibility, $V_{p_{aquifer}}$ is the aquifer pore volume, $\overline{p}_{aquifer}$ is the aquifer mean pressure, λ_{ij} is the connectivity between injection well and interface between aquifer and reservoir, $i_i(t)$ is injection rate, $e_w(t)$ is the water encroachment rate from the aquifer to the reservoir. For simplicity, the interface between the aquifer and transition zone is assumed as a single production well for the aquifer as the first porous medium and an injection well for the reservoir as the second medium. Hence, each injector well in the aquifer is related to the interface producer by a connectivity parameter λ_{ij}. The assumption of a single producer for the aquifer means $\lambda_{ij} = 1$. Consequently, Equation (5) is simplified as equation (6):

$$C_{taquifer}.V_{p_{aquifer}}\left(\frac{d\overline{p}_{aquifer}}{dt}\right) = \sum_{i=1}^{N_i} i_i(t) - e_w(t) \quad (6)$$

If water encroachment ($e_w(t)$) from the interface is considered as a single injection well for the production wells in the reservoir Equation (3 (CRMP)is rewritten as:

$$V_{pr}C_{tr}\left(\frac{d\overline{p}}{dt}\right) = f_j e_w(t) - q_j(t) \quad (7)$$

Merging equations (6) and (7):

$$V_{pr}C_{tr}\left(\frac{d\overline{p}}{dt}\right) = \left\{\left[f_j\sum_{i=1}^{N_i} i_i(t)\right] - \left(f_j C_{taquifer}.V_{p_{aquifer}}\frac{d\overline{p}_{aquifer}}{dt}\right)\right\} - q_j(t) \quad (8)$$

The pressure difference between reservoir mean pressure and aquifer mean pressure is defined as

$$D_P = \overline{P}_{aquifer} - \overline{P}_{reservoir} \quad (9)$$

If we assume the interface as a single point, then

$$V_{pr}C_{tr}\left(\frac{d\overline{p}}{dt}\right) = f_j I(t) - \left(f_j C_{taquifer}.V_{p_{aquifer}}\frac{d(\overline{p} + D_P)}{dt}\right) - q_j(t) \quad (10)$$

Equation (10) can be rewritten as

$$\left(V_{p_r}C_{tr} + f_j C_{taquifer}.V_{p_{aquifer}}\right)\left(\frac{d\overline{p}}{dt}\right) = f_j I(t) - f_j C_{taquifer}.V_{p_{aquifer}}\frac{dD_p}{dt} - q_j(t) \quad (11)$$

Coupling with the linear productivity index model (Equation (12) results in Equation (13)

$$q = j_{res}\left(\overline{p} - p_{wf}\right) \quad (12)$$

$$\left(\frac{V_{p_r}C_{tr} + f_j C_{taq}.V_{p_{aq}}}{J_{res}}\right)\left(\frac{dq_j}{dt}\right) + q_j(t) = f_j I(t) - f_j C_{taq}.V_{p_{aq}}\frac{dD_p}{dt} - \left(V_{p_{res}}C_{tres} + f_j C_{taq}.V_{p_{aq}}\right)\left(\frac{dP_{wf}}{dt}\right) \quad (13)$$

The time constant parameter (lag time) can be defined for reservoir and aquifer as

$$\tau_r = \frac{C_{tr}V_{p_r}}{J_{res}} \quad \tau_{aq} = \frac{C_{taq}V_{p_{aq}}}{J_{aq}} \quad (14)$$

Hence,

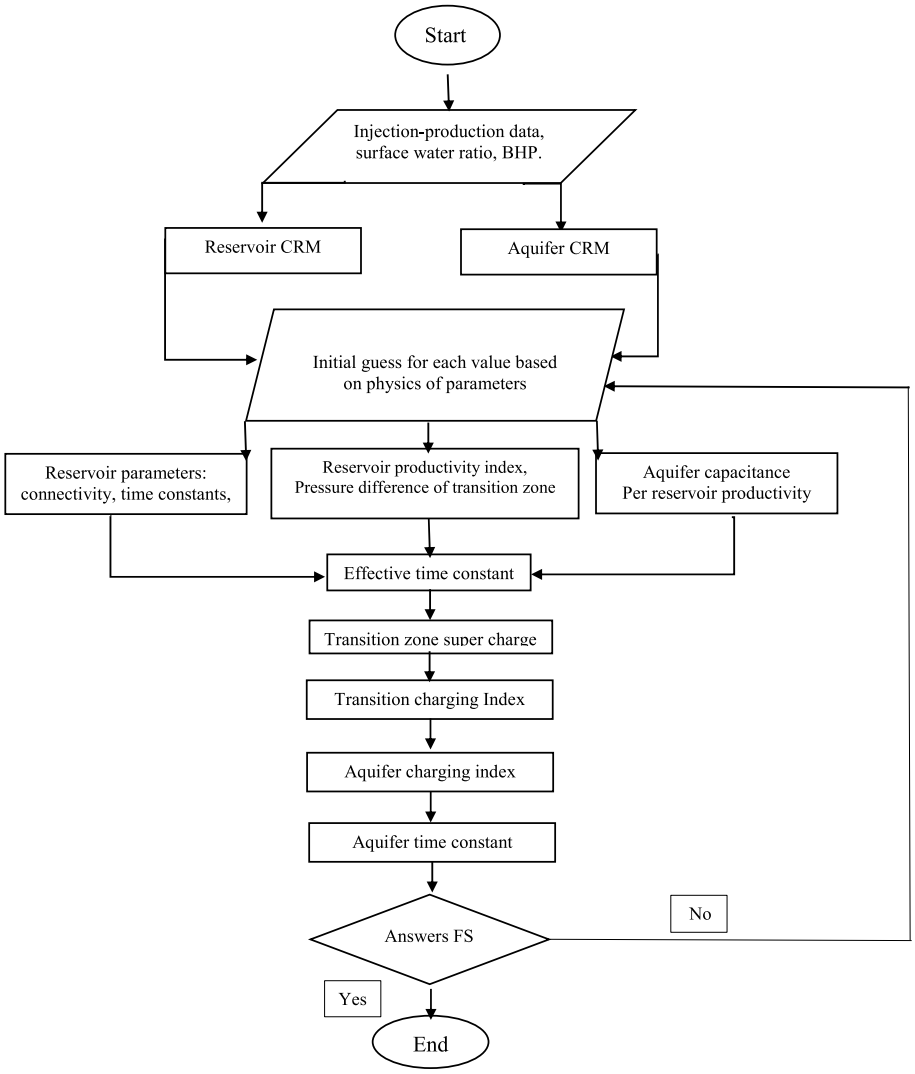


Fig. 4. Summary of the solution procedure.

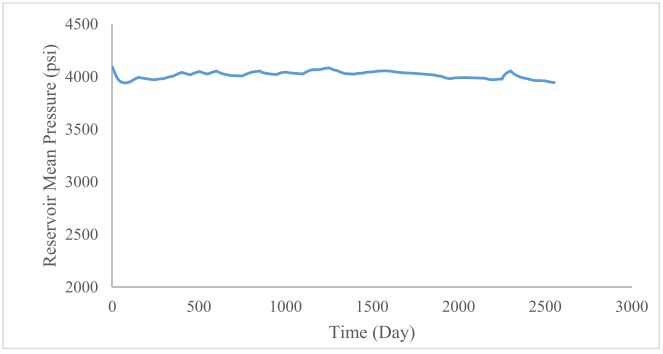


Fig. 5. Reservoir mean pressure while injecting water into the charging aquifer.

$$\left(\tau_r + \frac{f_j J_{aq} \tau_{aq}}{J_r}\right)\frac{dq_j}{dt} + q_j(t) = f_j I(t) - f_j J_{aq}.\tau_{aq}\frac{dD_p}{dt} - \left(\tau_r J_{res} + f_j J_{aq}.\tau_{aq}\right)\left(\frac{dP_{wf}}{dt}\right) \tag{15}$$

Consequently, the effective time constant is defined as:

$$\tau_{eff} = \tau_r + \frac{f_j J_{aq} \tau_{aq}}{J_{res}} \tag{16}$$

Therefore:

$$\frac{dq_j}{dt} + \frac{1}{\tau_{eff}} q_j(t) = \frac{f_j}{\tau_{eff}} I(t) - \frac{f_j J_{aq}.\tau_{aq}}{\tau_{eff}}\frac{dD_p}{dt} - J_{res}\left(\frac{dP_{wf}}{dt}\right) \tag{17}$$

Multiplying $e^{\int \frac{1}{\tau_{eff_j}} dt}$ as an integral factor at both sides of Equation (17).

$$e^{\int \frac{1}{\tau_{eff_j}} dt}\frac{dq_j}{dt} + \frac{e^{\int \frac{1}{\tau_{eff_j}} dt}}{\tau_{eff_j}} q_j(t) = \frac{f_j}{\tau_{eff_j}} e^{\int \frac{1}{\tau_{eff_j}} dt} I(t) - \frac{f_j J_{aq}.\tau_{aq}}{\tau_{eff_j}} e^{\int \frac{1}{\tau_{eff_j}} dt}\frac{dD_p}{dt} - J_{res} e^{\int \frac{1}{\tau_{eff_j}} dt}\frac{dP_{wf}}{dt} \tag{18}$$

So:

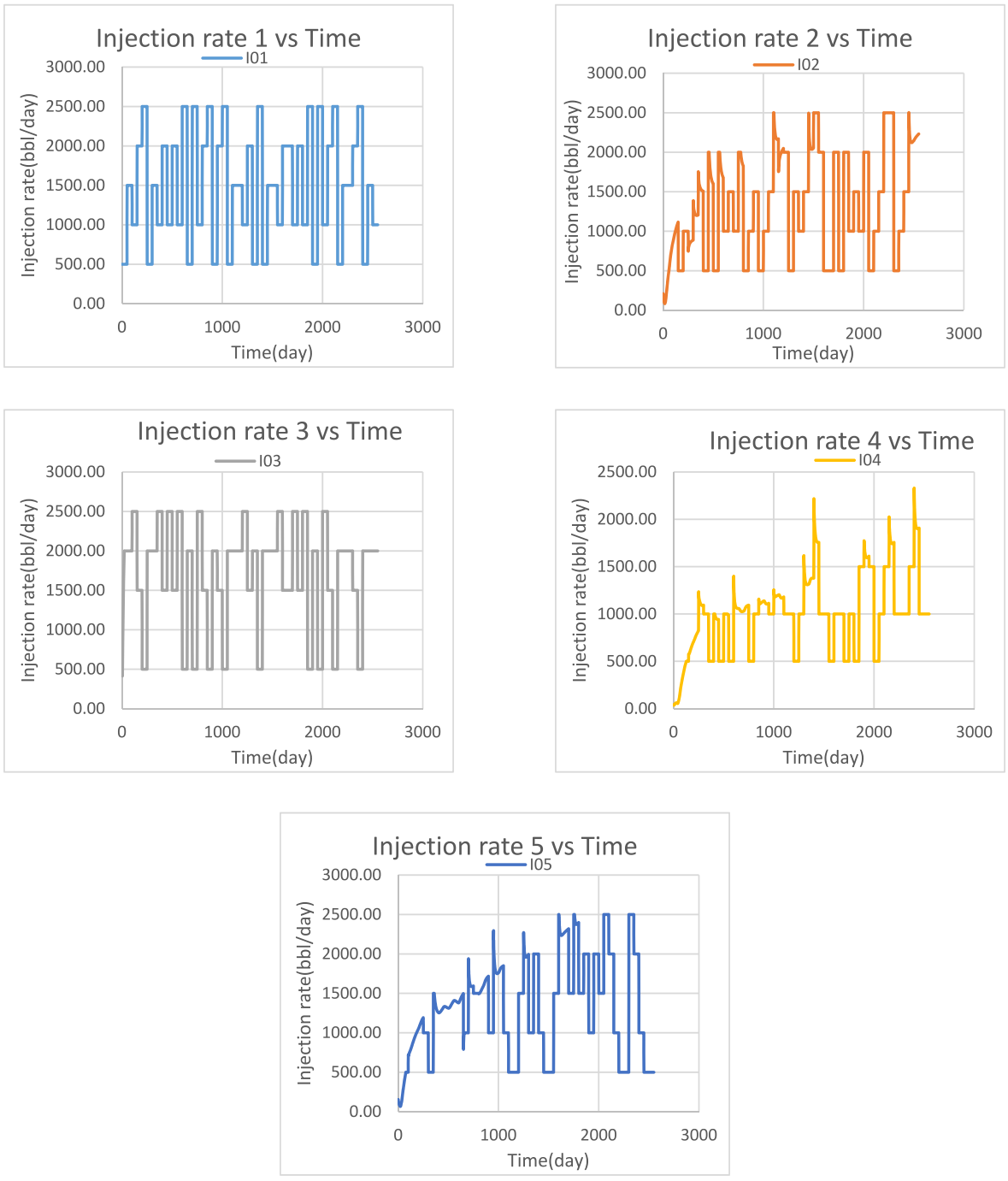


Fig. 6. Injection rates (Injection well No.1 to No.5) vs. time for homogenous case.

Table 1
SCRM reservoir and aquifer parameters for the homogenous case.

Well number	f_j %	$J_{res}\ \frac{RB}{Day.psi}$	$q(t_0)\ \frac{RB}{Day}$	$\frac{(CV)_{aq}}{J_{ress}}\ (Day)$	$\tau_{res}\ (Day)$	$\tau_{eff}\ (Day)$
P_1	0.26	6.88	2807.22	25.94	16.88	25.94
P_2	0.25	7.24	2913.51	23.33	16.04	23.33
P_3	0.25	6.63	2906.77	27.16	17.63	27.16
P_4	0.24	6.48	2893.34	26.46	17.99	26.46

Table 2
Calculated values of Pressure difference in the transition zone for the homogenous case.

Well number	DP (psi)						
	$0 \leq B_{s\&w} < 10$	$10 \leq B_{s\&w} < 20$	$20 \leq B_{s\&w} < 30$	$30 \leq B_{s\&w} < 40$	$40 \leq B_{s\&w} < 50$	$50 \leq B_{s\&w} < 60$	$60 \leq B_{s\&w} < 70$
P_1	10.66	10.19	9.64	9.20	8.72	8.24	8.24
P_2	10.52	9.99	9.46	8.62	8.18	7.79	0.00
P_3	10.50	9.95	9.46	8.99	8.48	8.01	8.01
P_4	10.41	9.95	9.54	9.07	8.68	8.02	0.00

Table 3
SCRM aquifer/reservoir interaction parameters for the homogenous case.

Well	Var.			
	$J_{transition}\left(\frac{RB}{Day.psi}\right)$	$J_{aq}\left(\frac{RB}{Day.psi}\right)$	$(CV)_{aq}\left(\frac{RB}{psi}\right)$	$\tau_{aq}\,(Day)$
P_1	31.33	8.81	116.06	13.17
P_2	35.83	9.07	116.09	12.79
P_3	31.08	8.44	116.97	13.87
P_4	33.40	8.04	116.58	14.50

$$\int_{t_0}^{t_n} \frac{d\left(e^{\int \frac{dt}{\tau_{eff_j}}} \times q_j\right)}{dt} dt = \frac{f_j}{\tau_{eff_j}} \int_{t_0}^{t_n} \left[e^{\int \frac{dt}{\tau_{eff_j}}} I(t)\right] dt - \frac{f_j J_{aq}.\tau_{aq}}{\tau_{eff_j}} \int_{t_0}^{t_n} \left[e^{\int \frac{dt}{\tau_{eff_j}}} \frac{dD_p}{dt}\right] dt - J_{res} \int_{t_0}^{t_n} \left[e^{\int \frac{dt}{\tau_{eff_j}}} \frac{dp_{wf}}{dt}\right] dt \tag{19}$$

Solving with part by part solution for the (t_{k-1}, t_k) time interval, $\frac{dI(t)}{dt}$ can be inferred as a slope of the line connecting injection rate at t_{k-1} to that of at t_k. Since the time interval of $(t_{k-1}.t_k)$ is small, the slope of the line is defined as $\frac{dI(t)}{dt} = \frac{\Delta I^k}{\Delta t_k}$; this concept can be repeated for the BHP as $\frac{dP_{wf}}{dt} = \frac{\Delta P_{wf}{}^k}{\Delta t_k}$;. Consequently, Equation (19) will be as follow:

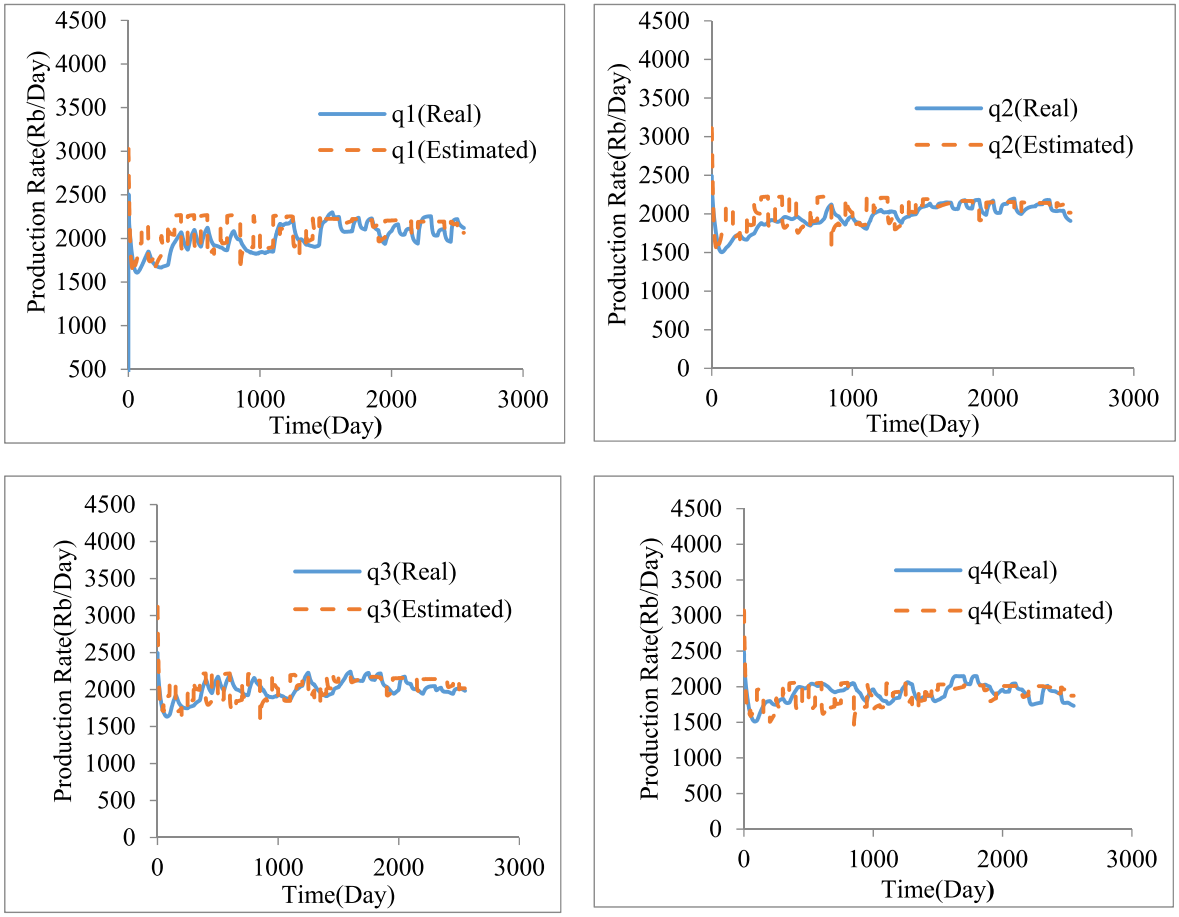


Fig. 7. Liquid rate estimation by SCRM and a fine-grid simulator for the homogenous case with aquifer charge.

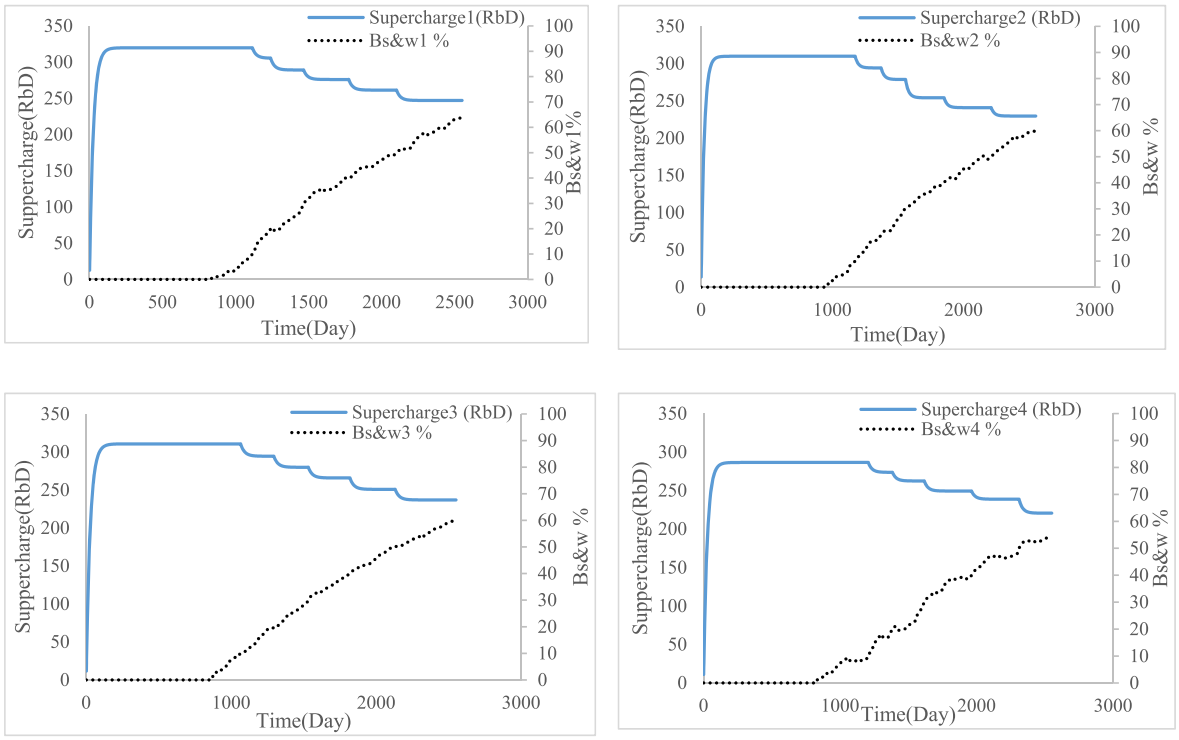


Fig. 8. Homogenous case supercharge between aquifer and production well drainage area in the reservoir and surface water.

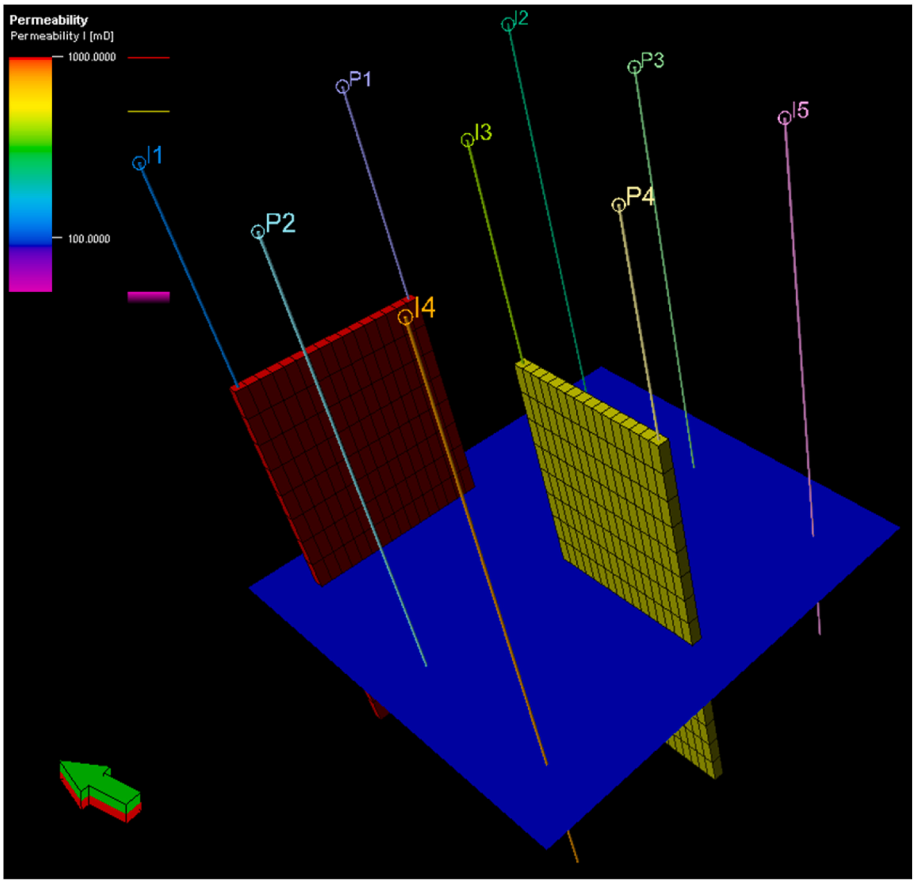


Fig. 9. Streak case schematic.

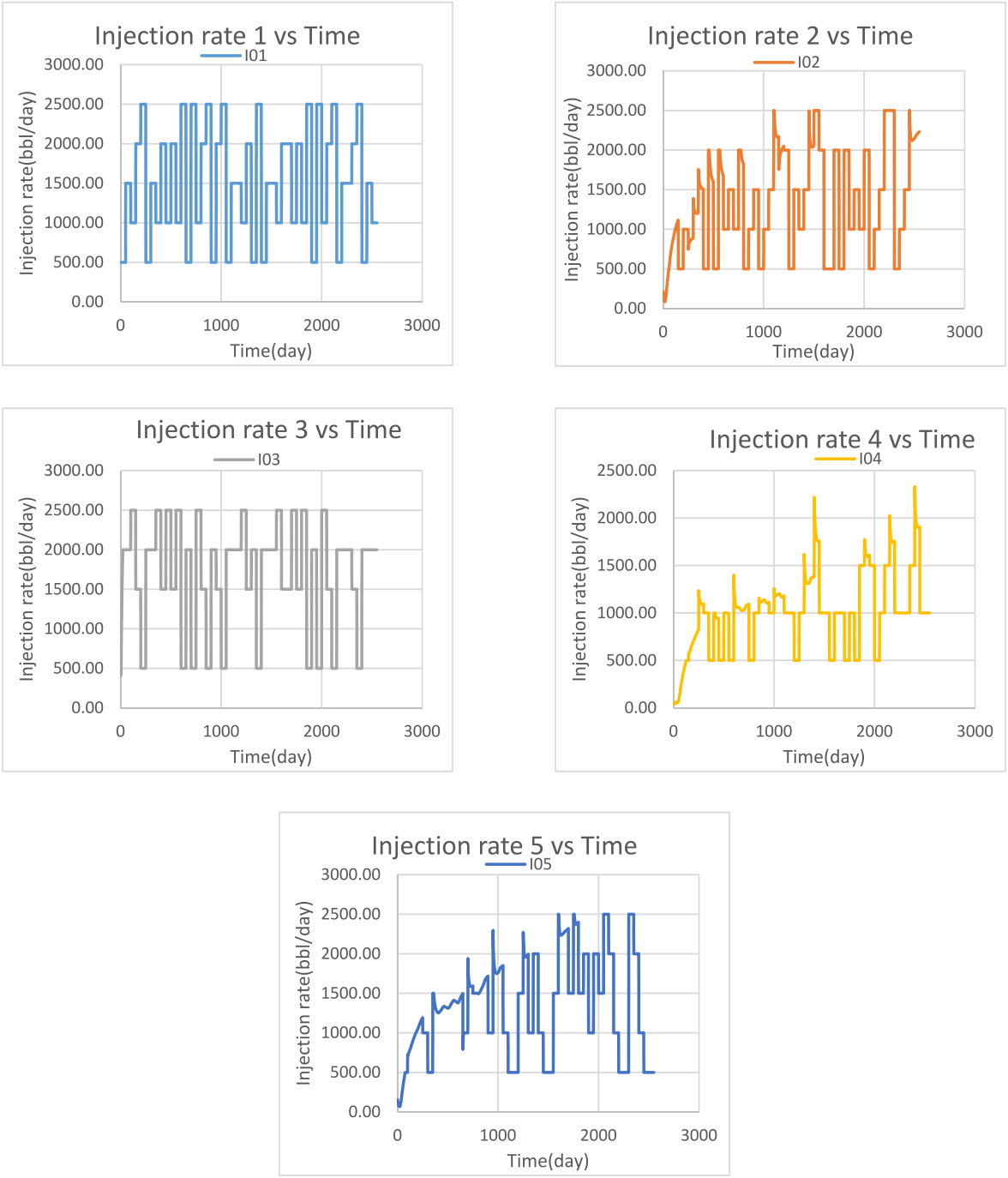


Fig. 10. Injection rates (Injection well No.1 to No.5) vs. time for streak case.

$$q_j(t_n) = q_j(t_0)e^{-\left(\frac{t_n - t_0}{\tau_{eff_j}}\right)} + f_j\left(I(t_n) - e^{-\left(\frac{t_n - t_0}{\tau_{eff_j}}\right)} I(t_0)\right) - e^{-\frac{t_n}{\tau_{eff_j}}} \sum_{k=1}^{n} \left\{ \left(e^{-\frac{t_k}{\tau_{eff_j}}} - e^{-\frac{t_{k-1}}{\tau_{eff_j}}}\right) \left(f_j \tau_{eff_j} \frac{\Delta I^k}{\Delta t_k} - J_{res_j} \tau_{eff_j} \frac{\Delta P_{wf}^{(k)}}{\Delta t_k} - f_j J_{aq} . \tau_{aq} \frac{\Delta D_p^{(k)}}{\Delta t_k}\right)\right\} \quad (20)$$

Equation (20) shows the modified CRMP where the last term indicates $q_{supercharge}$ as the spontaneous water influx occurs between aquifer and reservoir due to the pressure difference of aquifer and reservoir in the transition zone. Transition charging index ($J_{transition}$) and pressure difference in the transition zone develop an additional charge to the reservoir. It can be inferred that supercharge is the result of the pressure difference in the transition zone between the aquifer with 100% water and the reservoir with oil and water. Consequently, if water saturation in the reservoir increases, the reservoir pressure will be closer to the aquifer pressure and the aquifer/reservoir pressure difference can be neglected. In the other word, supercharge is the function of water saturation in reservoir zone and high water saturation in the reservoir equalizes the pressure in reservoir and aquifer zones; therefore, supercharge is affected adversely by increasing water saturation in the reservoir time. A mathematical expression is as

$$q_{supercharge} = J_{transition} \Delta p_{transition} \quad (21)$$

Hence, three control volumes are defined as aquifer with a charging index of J_{aq}, transition zone with a charging index of $J_{transition}$, and

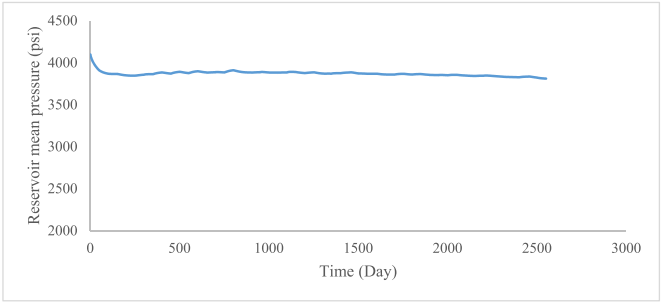


Fig. 11. Reservoir mean pressure while injecting water to the charging aquifer for streak case.

reservoir with a productivity index of J_{res}. The reservoir productivity index can be derived from aquifer and transition zone interaction. This concept has been established previously for the reservoir charging by constant pressure source by Ref. [9] as

$$\frac{1}{J_{res}} = \frac{1}{J_{aq}} + \frac{1}{J_{transition}} \tag{22}$$

As mentioned before, the interface of the aquifer and reservoir is assumed to be a single point. To estimate the pressure at the interface, we need to know the water saturation profile, which cannot be accurately estimated. We assumed that DP is a function of surface water cut (Bs&w), which is known. Injection/production history, surface water production, and bottom-hole pressure are considered as input data for the model. To solve Equation (20), an optimization algorithm is required to estimate DP as a function of surface water cut. Based on the surface water cut initial guess, other parameters such as well connectivity to interface, reservoir time constant, aquifer capacitance, and reservoir productivity index are calculated. To update the guess, the following objective function should be minimized. The GRG algorithm, which stands for "Generalized Reduced Gradient," has been implemented to minimize the objective function described below. In its simplest form, this solver method examines the gradient or slope of the objective function as the input values (also known as decision variables) change. It determines that an optimal solution has been reached when the partial derivatives equal zero. Among the nonlinear solving methods, GRG Nonlinear is considered one of the fastest optimization methods available for minimizing the total absolute error. Objective function will be defined as following equation including $q_j^{history}(t_k)$ production rate of numerical simulation at the each time step and $q_j^{SCRM}(t_k)$ is estimated production rate by developed SCRM at the each time step:

$$Obj\ function = \min \sum_{k=1}^{n} \sum_{j=1}^{n_p} \left| q_j^{history}(t_k) - q_j^{SCRM}(t_k) \right| \tag{23}$$

Hence, SCRM parameters including connectivity, reservoir time constant, reservoir productivity index, aquifer capacitance, and the difference between reservoir and aquifer mean pressure have been calculated. Other parameters such as effective time constant τ_{eff}, transition zone super charge, transition zone charging index (average value of transition zone super charge divided to average optimized value of pressure differences), and aquifer charging index are calculated. Summary of the solution procedure is represented in Fig. 4.

3. Results and discussion

This section simulated two synthetic reservoirs with charging aquifer support to verify the developed SCRM. Injection wells are completed in the charging aquifer zone for both cases, and production wells are completed in the reservoir. The physical description of the simulated models is shown in the following sections.

3.1. Homogenous model

The first model is a homogeneous reservoir charged by a homogeneous finite aquifer in which the aquifer pore volume is the same as the

Table 4
Calculated SCRM reservoir and aquifer parameters for the streak case.

Well number	f_{ij} %	$J_{res}\ \frac{RB}{Day.psi}$	$q(t_0)\ \frac{RB}{Day}$	$\frac{(CV)_{aq}}{J_{ress}}\ (Day)$	$\tau_{res}\ (Day)$	$\tau_{eff}\ (Day)$
P_1	48.92%	37.00	12530.25	2.72	2.73	4.06
P_2	4.72%	2.65	1400.19	204.12	28.15	37.77
P_3	3.53%	4.33	1264.13	215.01	26.38	33.97
P_4	42.83%	17.54	6869.18	7.54	6.65	9.88

Table 5
Calculated values of Pressure difference in the transition zone for the homogenous case.

Well	DP (psi)													
	Surface produced water range (%)													
	0–5	5–10	10–15	15–20	20–25	25–30	30–35	35–40	40–45	45–50	50–55	55–60	60–65	65–70	70–75
P_1	19	−2	−4	0	3	2	−11	−12	−6	5	5	2	0	4	5
P_2	10	8	7	7	7	6	6	_	_	_	_	_	_	_	_
P_3	16	12	11	11	10	7	_	_	_	_	_	_	_	_	_
P_4	13	0	1	0	−10	−3	0	2	2	4	2	4	4	1	3

Table 6
SCRM aquifer/reservoir interaction parameters for the streak case.

Well	Var.			
	$J_{transition}(RbD/psi)$	$J_{aquifer}\ (RbD/psi)$	$C_{aquifer}\ W_i\ (Rb/psi)$	$\tau_{aquifer}\ (Day)$
P_1	49.75	154.27	102.42	0.66
P_2	33.39	5.42	951.72	175.61
P_3	33.84	5.68	1046.33	184.09
P_4	56.29	25.43	132.16	5.20

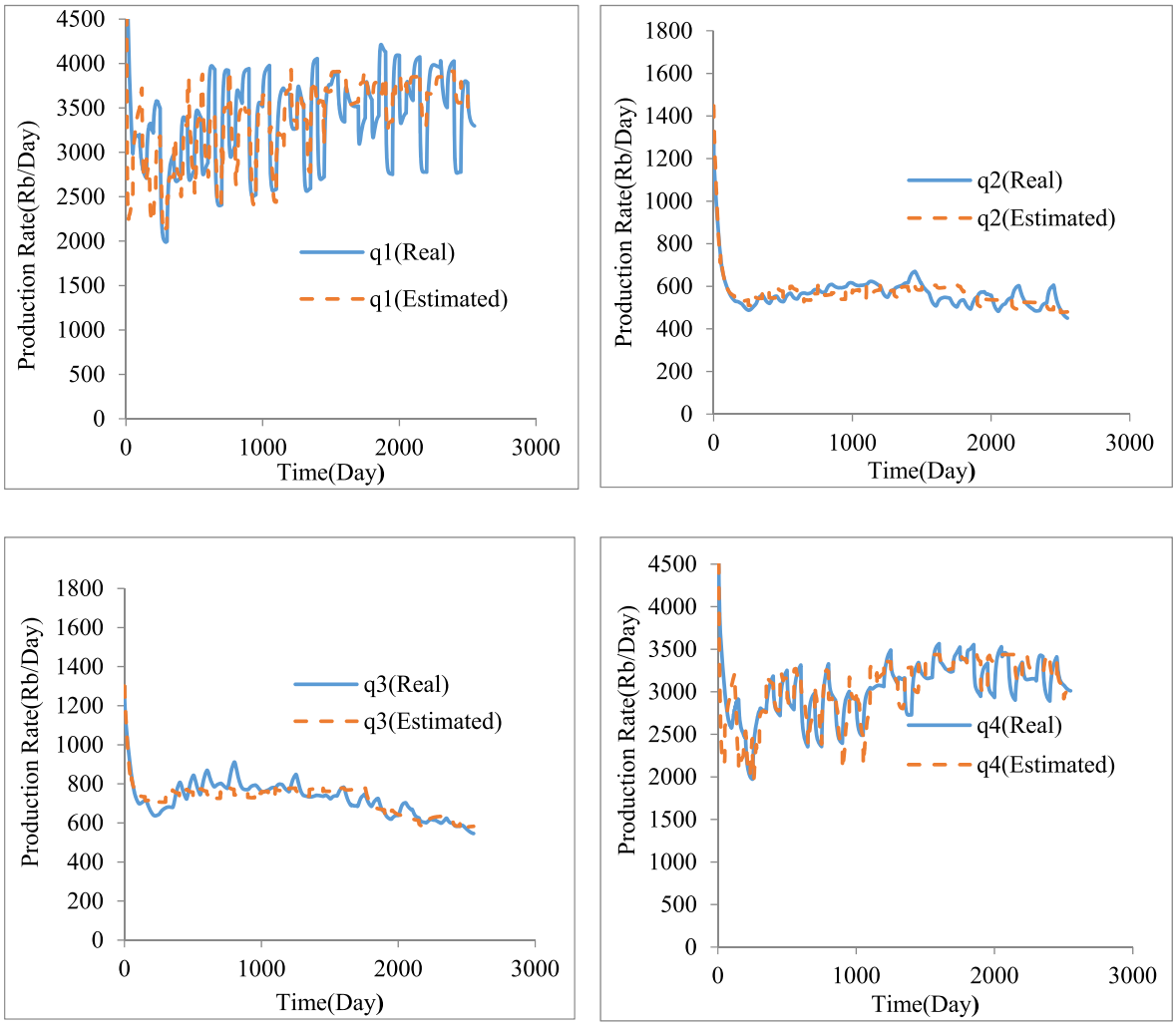


Fig. 12. Liquid rate estimation by developed SCRM and a fine-grid simulator for the streak case with aquifer charge.

reservoir. Five injection wells are located in the aquifer zone to maintain aquifer pressure ensuring a stable charge for the reservoir. Fig. 5 shows reservoir mean pressure history affected by pressure maintenance strategy. Furthermore, the reservoir produces through five wells with the same choke sizes at constant bottom hole pressure (BHP). The injection rate pattern of all five injectors is shown in Fig. 6. The porosity and permeability of the model are 0.25 and 100 md, respectively. Oil, water, and rock compressibility are $5\times10^{-6}\ \frac{1}{psi}$, $1\times10^{-6}\ \frac{1}{psi}$, and $1\times10^{-6}\ \frac{1}{psi}$, respectively.

Parameters including connectivity between interface and production wells, productivity index for each well, pressure differences as a function of surface water ratio for each production well, aquifer storage in each production well, and reservoir time constant for the production wells have been derived. Reservoir and aquifer parameters calculated by SCRM are shown in Table 1. Homogeneity of reservoir and aquifer is confirmed by the similarity of connectivity, aquifer storage, reservoir time constant, and productivity index values for all producers.

Table 2 shows the pressure differences as a function of $B_{s\&w}$. Because of a homogenous model with no significant event, pressure difference should reduce by increasing water saturation, which leads to a decrease in transition charge for each well. Moreover, these values should be in the same order, as shown in Table 2.

Based on the computed SCRM parameters, transition charge index and connectivity between aquifer and reservoir are estimated as shown in Table 3. Based on these data, the production of all wells is modeled by SCRM, as shown in Fig. 7, which shows an acceptable accuracy to estimate the production during pressure maintenance. The error of the estimation is about 6%.

Fig. 8 shows the change of surface water cut and its effect on the aquifer supercharge for all wells. Supercharge declines by producing more water that encroaches from the aquifer and reduces the pressure difference between the aquifer and the reservoir. In this case, the trend of supercharge for all wells is similar because of reservoir homogeneity.

3.2. Streak model

The volumetric streak case, developed by Ref. [8]; is a synthetic field consisting of five vertical injectors and four vertical producers. In this work, the streak case is simulated by considering charging aquifer to the reservoir. Two high-permeability streaks and well locations are displayed in Fig. 9. Except for two streaks, permeability is 100 md, elsewhere; porosity is assigned to be 0.25. Oil, water, and rock compressibility are $5\times10^{-6}\ \frac{1}{psi}$, $1\times10^{-6}\ \frac{1}{psi}$, and $1\times10^{-6}\ \frac{1}{psi}$, respectively. Constant BHP mode is considered for production wells in this model. Injection rates are shown in Fig. 10. Moreover, a pressure maintenance strategy has been performed to maintain reservoir mean pressure as a constant value, as shown in Fig. 11.

This synthetic model shows streak case of reservoir and aquifer which has two fractures with 1 Darcy (Red in Fig. 9) connecting first producer (P_1) and aquifer and 0.5 Darcy (yellow in Fig. 9) connecting the fourth producer (P_4); moreover, all of the injection wells are

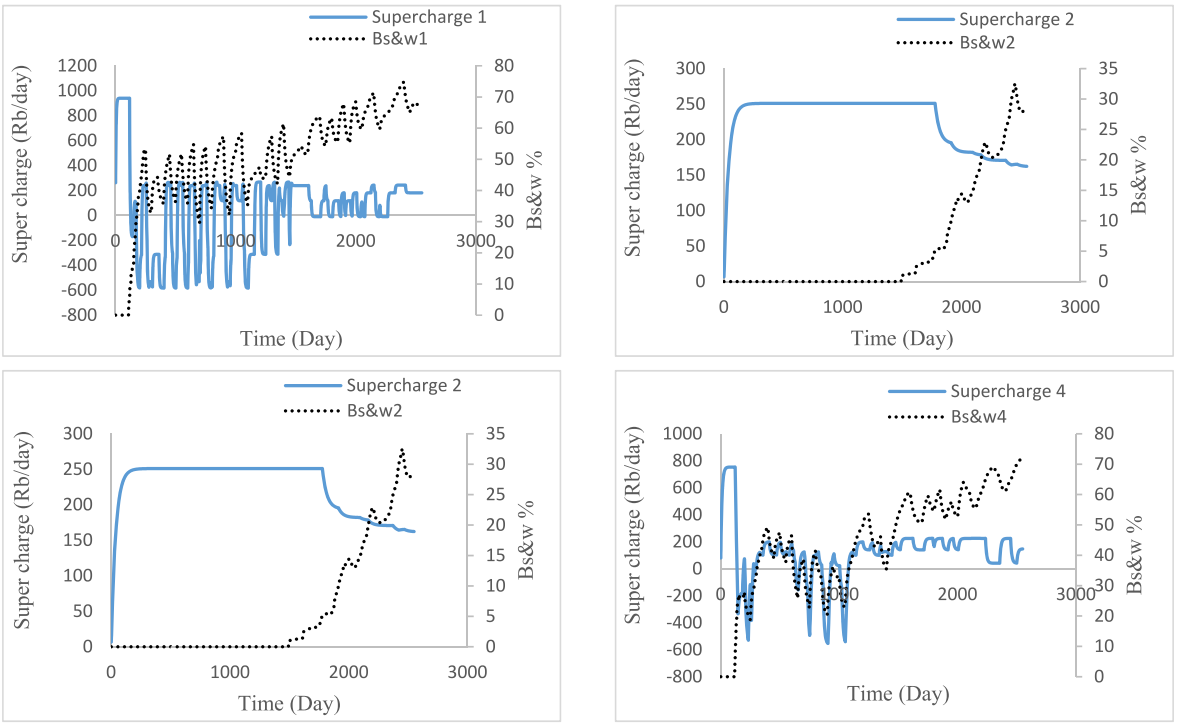


Fig. 13. Streak case supercharge between aquifer and production well drainage area in the reservoir and surface water.

completed in the aquifer zone and production wells in the reservoir.

Optimization parameters include connectivity between interface and production wells, productivity index for each well, pressure differences as a function of surface water ratio, aquifer storage in each production well investigation area, and reservoir time constant have been derived. Reservoir and aquifer parameters which have been calculated by developed SCRM, are provided in Table 4. Pressure differences in the transition zone as a function of Bs&w have been represented in Table 5. Supercharge is assumed to be a function of the surface water cut in 5% steps. A negative pressure difference value demonstrates reverse flow from the reservoir to the aquifer.

Based on the computed SCRM parameters, transition charge index and parameters showing the connectivity between aquifer and reservoir can be estimated as shown in Table 6. The developed SCRM has an acceptable accuracy in estimating pressure maintenance performance, as shown in Fig. 12.

As presented in Table 6 physical properties of reservoir and aquifer are shown by connectivity, aquifer storage, reservoir time constant, and productivity index value for each production well. According to the model, P_1 has 1000 md fracture at its drainage area. Our model shows the maximum value for the connectivity and productivity index and aquifer charging index for P_1, which is reasonable due to the presence of the fracture. P_2 and P_3 have the same reservoir properties without any fracture in the drainage area; consequently, connectivity and productivity index for P_2 and P_3 are the same and less than other wells. Because of lower permeability, aquifer and reservoir time constants for P_2 and P_3 is high.

Fig. 13 shows supercharge in the transition zone for all wells as a function of the surface water cut. P_2 and P_3 performance are like the homogenous case in which increasing in surface water cut means the reservoir water saturation increment and a decrease in transition zone charge rate. At early times of production, the surface water cut of well P_1 and P_4 shows fluctuation. We tried to simulate a model which has direct flow (from aquifer to the reservoir) and reverse flow (from reservoir to the aquifer), to show the capability of our method. In addition, the developed model can estimate injection performance by DP, which shows the values of mean reverse and direct flow based on its sign. Consequently, supercharge value of heterogeneous drainage area has been calculated in case either case of reverse or direct flow. If the surface water cut increases above 50%, supercharge demonstrates almost constant behavior and no reverse flow is observed. The optimization results in the streak case field show 7.5% relative error between estimation of developed SCRM and numerical simulator outputs.

4. Conclusion

A new method has been developed to simulate pressure maintenance scenarios by considering the water drive in which injection wells are completed in the aquifer. According to these implementations, the following points could be concluded.

The conventional CRM cannot be used to model reservoirs with aquifer support. New parameters should be added to the model to consider the pressure difference between the aquifer and reservoir transition zone (DP). This parameter is related to the reservoir water saturation. By producing water, this parameter is affected and decreases. By analyzing DP, aquifer/reservoir flow and reverse flow can be interpreted.

A new parameter is defined to shows the reservoir/aquifer interaction. In conventional CRM, leakage and charging effects are shown by the values of connectivity. Parameter DP, defined in this work, accurately estimates the flow between reservoir and aquifer and improves the performance of the CRM to model a reservoir under pressure maintenance condition.

Declaration of competing interest

The authors declare that they have no known competing financial interests or personal relationships that could have appeared to influence the work reported in this paper.

Data availability

Data will be made available on request.

References

[1] M. Sayyafzadeh, A. Mamghaderi, P. Pourafshari, M. Haghighi, A new method to forecast reservoir performance during immiscible and miscible gas-flooding via transfer functions approach, in: SPE Asia Pacific Oil and Gas Conference and Exhibition, 2011.

[2] M. Sayyafzadeh, P. Pourafshary, F. Rashidi, A novel method to model water-flooding via transfer function approach, in: SPE Project and Facilities Challenges Conference at METS, 2011.

[3] D. Weber, T.F. Edgar, L.W. Lake, L.S. Lasdon, S. Kawas, M. Sayarpour, Improvements in capacitance-resistive modeling and optimization of large scale reservoirs, in: SPE Western Regional Meeting, 2009.

[4] M. Sayarpour, Development and Application of Capacitance-Resistive Models to Water/carbon Dioxide Floods, The University of Texas at Austin, 2008.

[5] A. Albertoni, L.W. Lake, Inferring interwell connectivity only from well-rate fluctuations in waterfloods, SPE Reserv. Eval. \& Eng. 6 (2003) 6–16.

[6] A.A. Yousef, P.H. Gentil, J.L. Jensen, L.W. Lake, A capacitance model to infer interwell connectivity from production and injection rate fluctuations, SPE Reserv. Eval. \& Eng. 9 (2006) 630–646.

[7] L.W. Lake, X. Liang, T.F. Edgar, A. Al-Yousef, M. Sayarpour, D. Weber, Optimization of oil production based on a capacitance model of production and injection rates, in: Hydrocarbon Economics and Evaluation Symposium, 2007.

[8] M. Sayarpour, E. Zuluaga, C.S. Kabir, L.W. Lake, The use of capacitance–resistance models for rapid estimation of waterflood performance and optimization, J. Pet. Sci. Eng. 69 (2009) 227–238.

[9] M.J. Fox, A.C.S. Chedburn, G. Stewart, Simple characterization of communication between reservoir regions, in: European Petroleum Conference, 1988.

[10] D.B. Weber, The Use of Capacitance-Resistance Models to Optimize Injection Allocation and Well Location in Water Floods, The University of Texas at Austin, 2009.

[11] P.H. Gentil, The Use of Multilinear Regression Models in Patterned Waterfloods: Physical Meaning of the Regression Coefficients, 2005.

[12] A.A. Al-Yousef, Investigating Statistical Techniques to Infer Interwell Connectivity from Production and Injection Rate Fluctuations, The University of Texas at Austin, 2006.

[13] T.H. Kim, Improvement of reservoir management efficiency using stochastic capacitance resistance model, in: SPE Western Regional Meeting, 2019.

[14] B. Can, C.S. Kabir, Simple tools for forecasting waterflood performance, J. Pet. Sci. Eng. 120 (2014) 111–118.

[15] K.-H. Lee, A. Ortega, A.M. Nejad, I. Ershaghi, An active method for characterization of flow units between injection/production wells by injection-rate design, SPE Reserv. Eval. \& Eng. 14 (2011) 433–445.

[16] A.P. Nguyen, Capacitance Resistance Modeling for Primary Recovery, Waterflood and water-CO_2 Flood, 2012.

[17] B. Parekh, C.S. Kabir, Improved understanding of reservoir connectivity in an evolving waterflood with surveillance data, in: SPE Annual Technical Conference and Exhibition, 2011.

[18] A. Rezapour, T.A. Tafti, A. Ortega, I. Ershaghi, Injection scheduling design for reduced order waterflood modeling, in: SPE Western Regional \& AAPG Pacific Section Meeting 2013 Joint Technical Conference, 2013.

[19] M. Salazar, H. Gonzalez, S. Matringe, D. Castiñeira, Combining decline-curve analysis and capacitance-resistance models to understand and predict the behavior of a mature naturally fractured carbonate reservoir under gas injection, in: SPE Latin America and Caribbean Petroleum Engineering Conference, 2012.

[20] M. Soroush, D. Kaviani, J.L. Jensen, Interwell connectivity evaluation in cases of changing skin and frequent production interruptions, J. Pet. Sci. Eng. 122 (2014) 616–630.

[21] H. Wang, X. Liao, X. Dou, B. Shang, H. Ye, D. Zhao, C. Liao, X. Chen, Potential evaluation of CO2 sequestration and enhanced oil recovery of low permeability reservoir in the Junggar Basin, China, Energy \& fuels 28 (2014) 3281–3291.

[22] S.E. Eshraghi, M.R. Rasaei, S. Zendehboudi, Optimization of miscible CO2 EOR and storage using heuristic methods combined with capacitance/resistance and Gentil fractional flow models, J. Nat. Gas Sci. Eng. 32 (2016) 304–318.

[23] O. Izgec, C.S. Kabir, Quantifying reservoir connectivity, in-place volumes, and drainage-area pressures during primary depletion, J. Pet. Sci. Eng. 81 (2012) 7–17.

[24] R. Laochamroonvorapongse, C.S. Kabir, L.W. Lake, Performance assessment of miscible and immiscible water-alternating gas floods with simple tools, J. Pet. Sci. Eng. 122 (2014) 18–30.

[25] A.P. Nguyen, J.S. Kim, L.W. Lake, T.F. Edgar, B. Haynes, Integrated capacitance resistive model for reservoir characterization in primary and secondary recovery, in: SPE Annual Technical Conference and Exhibition, 2011.

[26] Z. Yin, C. MacBeth, R. Chassagne, O. Vazquez, Evaluation of inter-well connectivity using well fluctuations and 4D seismic data, J. Pet. Sci. Eng. 145 (2016) 533–547.

[27] A. Mamghaderi, A. Bastami, P. Pourafshary, Optimization of waterflooding performance in a layered reservoir using a combination of capacitance-resistive model and genetic algorithm method, J. Energy Resour. Technol. 135 (2013).

[28] G.A. Moreno, Multilayer capacitance–resistance model with dynamic connectivities, J. Pet. Sci. Eng. 109 (2013) 298–307.

[29] W.J. Al-Mudhafer, Parallel estimation of surface subsidence and updated reservoir characteristics by coupling of geomechanical \& fluid flow modeling, in: North Africa Technical Conference and Exhibition, 2013.

[30] W. Wang, T.W. Patzek, L.W. Lake, A capacitance-resistive model and InSAR imagery of surface subsidence explain performance of a waterflood project at Lost Hills, in: SPE Annual Technical Conference and Exhibition, 2011.

[31] W. Wang, others, Reservoir Characterization Using a Capacitance Resistance Model in Conjunction with Geomechanical Surface Subsidence Models, 2011.

[32] M. Almarri, B. Prakasa, K. Muradov, D. Davies, Identification and characterization of thermally induced fractures using modern analytical techniques, in: SPE Kingdom of Saudi Arabia Annual Technical Symposium and Exhibition, 2017.

[33] N. Naudomsup, L.W. Lake, Extension of capacitance/resistance model to tracer flow for determining reservoir properties, SPE Reserv. Eval. \& Eng. 22 (2019) 266–281.

[34] Q. Tao, S.L. Bryant, Optimizing carbon sequestration with the capacitance/resistance model, SPE J 20 (2015) 1094–1102.

[35] B. Prakasa, X. Shi, K. Muradov, D. Davies, Novel application of capacitance-resistance model for reservoir characterisation and zonal, intelligent well control, in: SPE/IATMI Asia Pacific Oil \& Gas Conference and Exhibition, 2017.

[36] M. Salehian, C. Temizel, I.M. Gok, M. Cinar, M.Y. Alklih, Reservoir management through characterization of smart fields using capacitance-resistance models, in: Abu Dhabi International Petroleum Exhibition \& Conference, 2018.

[37] C. Temizel, E. Artun, Z. Yang, Improving oil-rate estimate in capacitance/resistance modeling using the Y-function method for reservoirs under waterflood, SPE Reserv. Eval. \& Eng. 22 (2019) 1161–1171.

[38] R.W. de Holanda, E. Gildin, J.L. Jensen, A generalized framework for Capacitance Resistance Models and a comparison with streamline allocation factors, J. Pet. Sci. Eng. 162 (2018) 260–282.

[39] S.H. Yousefi, F. Rashidi, M. Sharifi, M. Soroush, A.J. Ghahfarokhi, Interwell connectivity identification in immiscible gas-oil systems using statistical method and modified capacitance-resistance model: a comparative study, J. Pet. Sci. Eng. 198 (2021), 108175.

[40] A. Mamghaderi, B. Aminshahidy, H. Bazargan, Error behavior modeling in Capacitance-Resistance Model: a promotion to fast, reliable proxy for reservoir performance prediction, J. Nat. Gas Sci. Eng. 77 (2020), 103228.

[41] W. Liu, W.D. Liu, J. Gu, A Machine Learning Method to infer inter-well connectivity using bottom-hole pressure data, J. Energy Resour. Technol. 142 (2020).

[42] D. Sen, Capacitance Resistance Model and Recurrent Neural Network for Well Connectivity Estimation: A Comparison Study, 2021 arXiv Prepr. arXiv2109.08779.

[43] A. Lesan, S. Ehsan Eshraghi, A. Bahroudi, M. Reza Rasaei, H. Rahami, State-of-the-art solution of capacitance resistance model by considering dynamic time constants as a realistic assumption, J. Energy Resour. Technol. 140 (2018).

[44] O. Izgec, Understanding waterflood performance with modern analytical techniques, J. Pet. Sci. Eng. 81 (2012) 100–111.

[45] O. Izgec, C.S. Kabir, Quantifying nonuniform aquifer strength at individual wells, SPE Reserv. Eval. \& Eng. 13 (2010) 296–305.

Nomenclature

Parameter

V_{pr}: Reservoir Pore Volume
$i_i(t)$: Injection rate of injection well i
$\bar{p}$: Reservoir Mean Pressure
J_{res}: Productivity Index
τ_r: Reservoir Time constant
$C_{t\,aquifer}$: Aquifer Total Compressibility
$\bar{p}_{aquifer}$: Aquifer Mean Pressure
D_p: Pressure difference of aquifer and reservoir
J_{aq}: Aquifer charging Index
$I(t)$: Sum of injection rate for the injectors
$q_{supercharge}$: Charging due to pressure difference
$B_{s\&w}$: Surface produced water ratio
C_{tr}: Reservoir Total Compressibility
$q_j(t)$: Production rate of producer j
p_{wf}: Well flow Pressure
f_{ij}: connectivity between injector i and producer j
$V_{P\,aquifer}$: Aquifer Pore Volume
λ_{ij}: Injectors connectivity and interface of reservoir and aquifer
$e_w(t)$: Water encroachment of aquifer
τ_{aq}: Aquifer Time constant
τ_{eff}: Effective time constant of aquifer/reservoir complex
$J_{transition}$: Transition zone charging Index
$\Delta p_{transition}$: Transition zone pressure difference